



HAL
open science

Catalytic Injectors for an Isochoric Hybrid Rocket Motor

Antony J. Musker, Jean-Yves Lestrade, Jérôme Anthoine, Anthony Lécossais

► **To cite this version:**

Antony J. Musker, Jean-Yves Lestrade, Jérôme Anthoine, Anthony Lécossais. Catalytic Injectors for an Isochoric Hybrid Rocket Motor. *Space Propulsion* 2018, May 2018, SEVILLE, Spain. hal-02003092

HAL Id: hal-02003092

<https://hal.science/hal-02003092v1>

Submitted on 1 Feb 2019

HAL is a multi-disciplinary open access archive for the deposit and dissemination of scientific research documents, whether they are published or not. The documents may come from teaching and research institutions in France or abroad, or from public or private research centers.

L'archive ouverte pluridisciplinaire **HAL**, est destinée au dépôt et à la diffusion de documents scientifiques de niveau recherche, publiés ou non, émanant des établissements d'enseignement et de recherche français ou étrangers, des laboratoires publics ou privés.

Catalytic Injectors for an Isochoric Hybrid Rocket Motor

Antony J. Musker¹, Jean-Yves Lestrade², Jérôme Anthoine², Anthony Lécossais³

¹ DELTACAT Ltd, Kintyre House, 70 High Street, Fareham, Hampshire, PO16 7BB, UK.
Visiting Professor, Aeronautics and Astronautics Unit, University of Southampton, UK, Email:
tony.musker@deltacatuk.com

² ONERA / DMPE, Université de Toulouse, F-31410 Mauzac, France

³ Airbus Defence and Space, F31400 Toulouse, France



ABSTRACT

The EU H2020 HYPROGEO Project [1], coordinated by Airbus Defence and Space (Toulouse), called for the design and manufacture of two sets of catalytic injectors for a novel, isochoric hybrid rocket motor. The hybrid motor forms the basis of a propulsion system for future GEO/apogee-kick applications. The motor burns its fuel axially rather than radially and relies on a constant, vortical flow of hot oxygen for ignition and sustained combustion. The hot oxygen is provided by the rapid decomposition of hydrogen peroxide. Two aqueous concentrations were used: 87.5% for an intermediate motor, and 98% for the final breadboard design [2]. Critical to success is the catalyst, referred to as PX1. This comprises a ceramic substrate and an active (catalytic) surface. On contact with hydrogen peroxide, oxygen and steam are liberated exothermically. The efficacy of PX1, used in combination with 98% concentration peroxide, was demonstrated in 2016 [3].

Each catalytic injector system comprises six decomposition chambers and six injector ducts. The peroxide is fed into the decomposition chambers, which are filled with PX1 pellets. The ensuing hot oxygen is then directed into the injector ducts, which connect to an injector ring. The injector ring is positioned just below the base of a cylindrical fuel grain. The fuel grain used is high density polyethylene. On contact with the fuel grain, ignition and sustained combustion follow.

A significant difficulty in designing the injector ducts was associated with the need for the hot

oxygen to be vectored such that the hot gas flowed tangentially rather than radially with respect to the fuel grain's axis. This vortical flow pattern enhances mixing by increasing the hot-gas residence time in the combustion chamber; it also helps to maintain isochoric conditions within the combustion chamber, thereby maintaining a reasonably constant thrust. It was found that the ducts could not easily be designed for subsequent manufacture using a traditional 5-axis milling machine. Instead the ducts were 3D-printed. For use with 98% peroxide, the chosen duct material was Inconel 625.

The paper describes the design of the catalytic injectors and the interfaces with the combustion chamber. Relevant test data are also presented, together with the method of quantifying the axial regression rate of the fuel grain in terms of the injector parameters.

NOMENCLATURE

a	Regression law coefficient
α	defined angle
θ	defined angle
D	Internal diameter of combustion chamber
g	Acceleration due to gravity
G_{ox}	Mass flux of HTP product gases over all injector ducts
h	Height of each rectangular-section injector duct
I_{sp}	Vacuum specific impulse
k	Number of pairs of data points for regression analysis
m	Regression law exponent

M_r	Mass mixture ratio (HTP:fuel)
dm_{ox}/dt	Total mass flow-rate of HTP over all injector ducts
dm_f/dt	Mass flow-rate of fuel
n	Number of injector ducts
ρ_f	Density of HDPE fuel
Q	Sum of squared residuals in calculation of a and m
T	Vacuum thrust
t	time
w	Cross-sectional width of exit of injector duct
dx/dt	Averaged axial regression rate of fuel grain
x_i	i 'th value of HTP mass flux
y_i	i 'th value of fuel regression rate

Acronyms

ALM	Additive Layer Manufacturing (or 3D printing)
HDPE	High density polyethylene
HTP	High Test Peroxide (rocket-grade hydrogen peroxide)
PX1	Chosen catalyst for HYPROGEO

1. INTRODUCTION

One of the difficulties of using hybrid motors for GEO applications is that they tend to be long and slender. This type of geometry places considerable and undesirable constraints on the layout of the satellite or spacecraft. HYPROGEO has focused on developing a demonstrator hybrid motor that has a length-to-diameter ratio of the order of 1 rather than 10 or more. Another difficulty with conventional hybrid motors is that the effective volume of the 'combustion chamber' increases with burn time; this leads to a constantly reducing thrust. HYPROGEO uses an isochoric (constant-volume) combustion chamber. This is achieved by burning the fuel axially (end-grain burning) rather than radially.

The motor uses high density polyethylene and high-purity, 98% concentration hydrogen peroxide. Combustion occurs in two stages. The peroxide passes through a number of

decomposition chambers, which are filled with PX1 catalytic pellets. The peroxide is then reduced to steam and oxygen at a temperature of the order of 900 deg C. These gases are then directed into the combustion chamber by a series of injection ducts such that they skim the surface of the fuel grain; this causes ignition and sustained combustion of the fuel. The decomposition chambers and injection ducts are referred to as the 'catalytic injector'. As the fuel grain burns, it is moved axially by a pressure device such that the burning surface is kept in a constant position with respect to the incoming stream of hot oxygen.

The injection conditions are set by several factors; these include oxidiser mass flow-rate, gas speed, direction, temperature and pressure. Critical to successful operation of the engine is the device used to inject the hot oxygen (and steam) into the combustion chamber.

The design methodology and analysis are described in Sections 2 and 3. Section 4 presents some results from our initial firings. The conclusions are presented in Section 5.

2. DESIGN METHODOLOGY

Several options were assessed for the critical oxidiser injection process. The one selected calls for a number of decomposition chambers to be fed with HTP by means of a series of flexible hoses. These hoses are connected to the propellant delivery rig via a distributor. These decomposition chambers are welded directly to the combustion chamber's mechanical interface using a series of injector ducts, as shown in Figure 1. Each injector

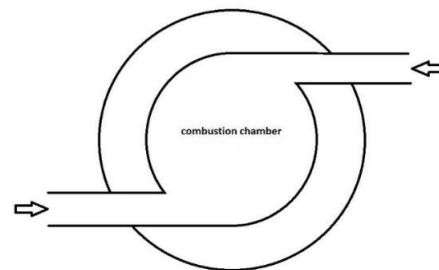


Figure 1. Concept Image of Injector Arrangement (viewed along thrust axis)

duct is in turn welded to its own decomposition chamber. In this way, the hot oxygen is directed into the combustion chamber at an angle (to be chosen), creating a swirling motion inside the

chamber. In a sense, the catalytic injector becomes a hot-oxygen vortex generator, with the axis of the vortex directed towards the exhaust nozzle. This concept will be described in detail in the next section.

3. IDEALISED ANALYSIS

When designing a *classical*, radially-burning, hybrid rocket, the regression rate is usually described in its simplest form by the following equation:

$$dx/dt = aG_{ox}^m \quad (1)$$

where dx/dt is the axial fuel radial regression rate, G_{ox} is the mass flux based on cross-sectional area of the internal diameter, a is an empirical constant, depending on the propellant chemistry, and m is an empirical exponent. Whereas the flow in a classical hybrid is described by an axial, developing, thermal boundary layer with a diffusion flame, for the HYPROGEO concept the entry flow of the oxidiser is radial (perpendicular to the thrust axis). Consequently, the regression rate is likely to be highly variable across the burning surface. Moreover, enhanced radiation effects within the combustion chamber will most likely reduce the regression rate, which would weaken the mixture ratio and reduce the achieved characteristic velocity and specific impulse.

Although the value of the exponent, m , depends on the unknown radiation component, its convective value is thought likely to be little different from the classical case (perhaps nearer unity). Therefore, in the absence of anything better, the following analysis has proceeded using the classical law.

The design of the intermediate catalytic injector starts with a simple geometrical analysis to identify the size of the injection ports in terms of the angle of entry and required HTP mass flow-rate. This is best explained by reference to Figures 4 and 5 (the latter shows just a single injector duct). Here, the decomposed HTP gases enter the (hot-oxygen) injector duct at A. The duct has width w and height h (h is parallel to the thrust axis). The mass flow rate of gas for this isolated duct is thus ρUhw , where ρ is the gas density, found from thermo-chemical calculations, and U is the gas speed. A critical factor for efficient injection is the angle of entry, α , defined as the angle ABE. For radial entry, $\alpha = 90$ degrees; for tangential entry, α is zero. The angle subtended by the injector port, θ , is

defined by BCF. Analysis of this geometry leads to:

$$w = D \sin(\theta/2) \cdot \sin(\alpha + \theta/2) \quad (2)$$

where D is the internal diameter of the combustion chamber. So, for a selected entry angle, α , the duct width, w , is defined. The angle θ needs to be set to the circumference of the combustion chamber's inner diameter divided by an integer, n , where n is the number of injector ducts.

After some pilot CFD studies, which will not be described here, it was clear that a tangential entry was preferable to a radial entry. Other values led to extensive 'hot spots' on the wall of the combustion chamber. Consequently, it was decided at an early stage to set α to zero.

The following analysis focuses on the design values of n , w and h .

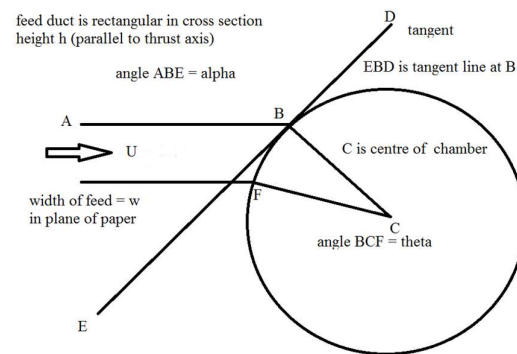


Figure 2. Geometry for a Single Injector Duct (viewed along thrust axis)

Firstly, assuming perfect nozzle expansion, the thrust is given by:

$$T = (dm_t/dt) g I_{sp} \quad (3)$$

where $dm_t/dt = dm_{ox}/dt + dm_f/dt$

Hence: $dm_t/dt = (dm_{ox}/dt) (1 + 1/M_r)$

and $dm_{ox}/dt = T \{g I_{sp} (1 + 1/M_r)\}^{-1}$

The regression rate is assumed to be described by:

$$dx/dt = a (G_{ox})^m \quad (4)$$

where $G_{ox} = (dm_{ox}/dt)/(nwh)$

and a and m are empirical constants.

Therefore:

$$dx/dt = 4 (dm_{ox}/dt)/(\pi D^2 M_r \rho_f) \quad (5)$$

Eqs. (6) and (7) give:

$$\begin{aligned} & 4 (dm_{ox}/dt)/(\pi D^2 M_r \rho_f) \\ & = a \{(dm_{ox}/dt)/(nwh)\}^m \end{aligned} \quad (6)$$

Using the geometrical constraint on w that must be satisfied in Eq. 2:

$$w = D \sin(\theta/2) \times \sin(\alpha + \theta/2)$$

For tangential entry, α must be zero. So:

$$w = D \sin^2(\theta/2)$$

The total injection cross-sectional area = nwh , where n is the number of injector ducts. So Eq. 6 becomes:

$$\begin{aligned} & 4(dm_{ox}/dt)/(\pi D^2 M_r \rho_f) \\ & = a \{(dm_{ox}/dt)/[nhD \sin^2(\theta/2)]\}^m \end{aligned} \quad (7)$$

Note that to avoid hot spots between the injector ports, which could cause melt-down of the interface ring or even of the lower part of the fuel grain, the gaps between the injector ports must be very small. In the limit $\theta = 2\pi/n$ radians (for $n \geq 4$).

Re-arranging equation (7):

$$h = (1/n)\{A/B\}^{(1/m)} \quad (8)$$

where $A = a\pi\rho_f M_r D^{(2-m)}$

and $B = 4(dm_{ox}/dt)^{(1-m)} \sin^{2m}(\pi/n)$

subject to the strict condition in Eq. (3) that:

$$dm_{ox}/dt = T \{g I_{sp} (1 + 1/ M_r)\}^{-1}.$$

Finally, the duct height, h , is given by:

$$\frac{(a\pi\rho_f M_r)^{\frac{1}{m}} D^{(2-m)/m} \{g I_{sp} (1 + \frac{1}{M_r})\}^{\frac{1-m}{m}}}{4^{1/m} T^{(1-m)/m} n \sin^2(\frac{\pi}{n})} \quad (9)$$

For a required thrust and specific impulse, Eq. 9 defines the all-important height to be used for the injector ducts, expressed in terms of the various engine parameters. The values of a and m to be used for the final design were based on data recorded from a smaller, pilot series of experiments.

The above analysis shows that as the mixture ratio decreases (7.4 is the optimum value for HDPE/98% HTP), the oxidiser mass flux must increase but with a *low* mass flow-rate. This places limits on achievable thrust. This is

counter-intuitive, in that to achieve a low mixture ratio a *high* mass flow-rate of fuel is needed; in turn this demands a high max flux. But the mass flux is controlled by both the HTP mass flow-rate *and* the associated cross-sectional area of the combined injector ducts.

The final choice of a and m was made using regression data from a pilot experiment that used 87.5% concentration HTP. The following simple analysis can be used to determine a and m and hence to size the injector ducts using Eq.9.

The regression rate is assumed to be described by equation 1:

$$dx/dt = a (G_o)^m$$

where G_o is now $(dm_{ox}/dt)/(nwh)$ and (nwh) represents the total exhaust area of all n injector ducts.

Let i 'th regression rate measurement = y_i

Let i 'th mass flux measurement $(G_{ox})_i = x_i$.

Let there be k pairs of experiment data.

Let Q represent the sum of the squared residuals. We require to find the values of a and m associated with a minimum value of Q :

$$Q = \sum_{i=1}^k (y_i - ax_i^m)^2 \quad (10)$$

When Q is a minimum:

$$\partial Q/\partial a = 0; \quad \partial Q/\partial m = 0.$$

$$\partial Q/\partial a = \partial/\partial a \sum_{i=1}^k (y_i^2 + a^2 x_i^{2m} - 2y_i a x_i^m) = 0$$

$$\text{hence } a = \frac{\sum_{i=1}^k (y_i x_i^m)}{\sum_{i=1}^k (x_i^{2m})} \quad (11)$$

and

$$\partial Q/\partial m = \partial/\partial m \sum_{i=1}^k (y_i^2 + a^2 x_i^{2m} - 2y_i a x_i^m) = 0$$

$$= -2 \sum_{i=1}^k \{(y_i - a x_i^m) a x_i^m \log(x_i)\}$$

Hence $m =$

$$\left\{ \sum_{i=1}^k \log(x_i) \right\}^{-1} \left\{ \sum_{i=1}^k \log(y_i) - k \log(a) \right\} \quad (12)$$

Combining Eqs.3 and 4:

$$m = \left\{ \frac{\sum_{i=1}^k \log(y_i)}{k \log \left(\frac{\sum_{i=1}^k (y_i x_i^m)}{\sum_{i=1}^k (x_i^{2m})} \right)} \right\} / \left\{ \sum_{i=1}^k \log(x_i) \right\} \quad (13)$$

Using the pilot data, with 87.5% HTP, the values of a and m were found to be $4.04 \times 10^{-5} \text{ kg}\cdot\text{m}^{(2m+1)}\text{s}^{(m-1)}$ and 0.27 respectively.

The observed variation between regression rate and HTP mass flux, G_{ox} , is shown in Figure 1. It can be seen that Eq.1 describes the trend in the observed data reasonably well. Note that the uncertainty in the measured mass flow-rate of fuel, and hence regression rate, is rather poor, because some fuel is lost by thermolysis during the (monopropellant) warming phase.

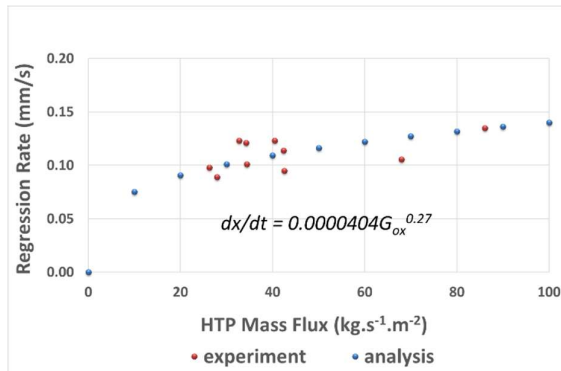


Figure 3. Regression rate versus HTP mass flux.

Figure 2 shows the variation of HTP mass flow-rate with mixture ratio, showing that for a desired mixture ratio and thrust, which is set by the total mass flow-rate, the fuel mass flow-rate is fixed. Since the fuel regression rate is also fixed by Equation 1, the fuel-grain diameter is fixed by the target thrust. It will be seen that the above analysis represents the cornerstone of the design process. Note that the optimum mixture ratio for HDPE and 98% HTP is 7.4.

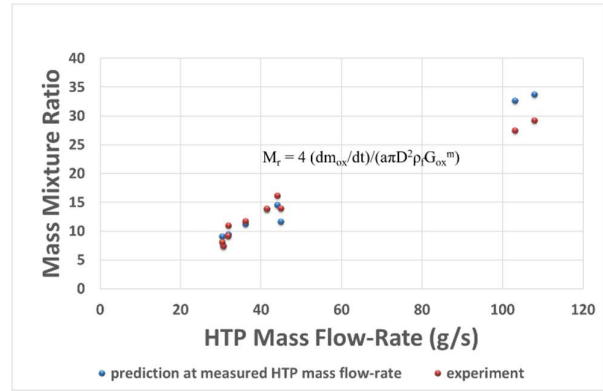


Figure 4. Mixture Ratio versus HTP Mass Flow-Rate.

4. DESIGN CONSIDERATIONS

The final demonstrator engine was designed to meet the following design targets:

- a. total throughput of 98% HTP = 200 kg
- b. 98% HTP mass flow-rate = 52 g/s
- c. design CC pressure = 8.8 bar absolute
- d. design thrust, $T = 187 \text{ N}$
- e. nozzle throat diameter = 11.5 mm (tentative at the time of writing)
- f. number of injector ducts = 6, operating at approximately 950 deg C
- g. combustion chamber diameter = 250 mm

It should be noted that in practice, due to uncertainties, the HTP flow-rate would most likely need to be adjusted to achieve the optimum engine performance.

Decisions were taken during the design of the catalytic injector to ensure that the above criteria were met. The desired mixture ratio for optimal performance was cited in Section 3 as 7.4. This was calculated using both CEA2 and Cpropep, which follow the method of Gordon and McBride.

Each of the 6 catalytic injectors comprises an inlet manifold, an injector plate, a decomposition chamber, a retainer plate and an injector duct.

The geometry for the decomposition chambers was found using the methodology described by Musker and described in [3]. This attempts to specify the geometry such as to ensure that the

total throughput of 98% HTP (200 kg) is achievable. For the given design total mass flow-rate of HTP (52 g/s), each decomposition chamber must supply 8.7 g/s. This corresponds to a nominal bed loading of $9.8 \text{ kg}\cdot\text{s}^{-1}\cdot\text{m}^{-2}$ for the PX1 catalyst. A safety factor of 2 was used, meaning that in practice the combined decomposition chambers ought to be able to handle 400 kg of HTP. In this way, the length of each decomposition chamber was set at 103.7 mm, allowing the chamber to be used at the upper limit of HTP mass flow-rate specified by ONERA. The elastic safety factor for the hoop stress is 11.3, based on the 0.2% yield stress of Inconel 625 at an operating temperature of 950 deg C.

Three injector plates were manufactured, each designed to operate within a specified flow-rate. The chosen injector plate is sealed by means of Viton O rings on both sides. These sit in grooves machined in both the inlet manifold and the upstream end of the decomposition chambers.

The six injector ducts are welded to the injector ring, which sits between the combustion chamber's main flanges. The job of the injector ducts is to convey the hot oxygen and steam from the decomposition chambers into the combustion chamber in such a way as to impart a vortex of hot, oxygenated gas across the fuel grain.

The value of h chosen for manufacturing the ducts was 5.0 mm. During the tests, h can be made smaller by the use of inserts (clearly, it cannot be made larger). The mechanical interface is designed to allow a series of inserts to be positioned against the ducts' exhausts, which reduce the effective value of h , thus controlling the HTP mass flux. The width of the duct's exit slot, w , is set by the circumference of the combustion chamber divided by 6. In practice, the width is somewhat shorter due to the thickness of the duct walls. A value of 55 mm was chosen, thus providing a minimum HTP mass flux of $31.5 \text{ kg}\cdot\text{s}^{-1}\cdot\text{m}^{-2}$ at the target HTP mass flow-rate (without the use of inserts).

ONERA's mechanical interface design for the BB is shown in Figure 11. A typical insert is shown in Figure 12.

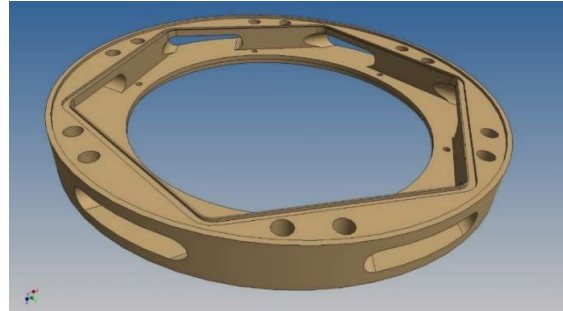


Figure 5. ONERA's Design for the Mechanical Interface.

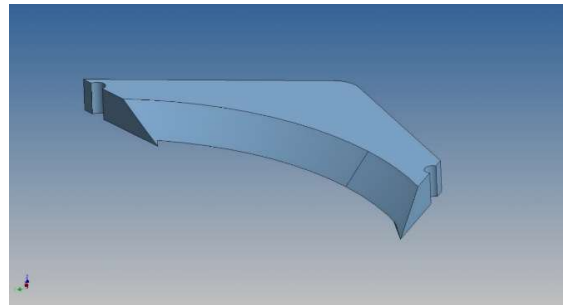


Figure 6. Typical Insert to be Used to Control the Mass Flux (from ONERA).

The duct's wall thickness at the exhaust end was modelled using a simple, linear hex finite element computer code. The exhaust end was considered to be the most stressed region because of the large width-to-height ratio (w/h). The temperature in this region was estimated to be 900 deg C.

Knowing the appropriate wall thickness to use from the finite element analysis, and the end constraints imposed by the decomposition chamber and the mechanical interface, the geometry of the injector duct was defined using bi-cubic splines. The injector duct is shown in Figures 16 and 17. Various views of the assembly are shown in Figures 19-23.

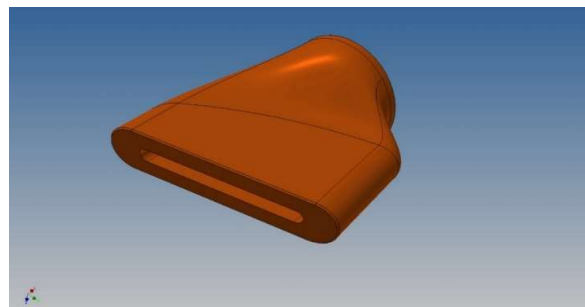


Figure 7. BB Injector Duct.

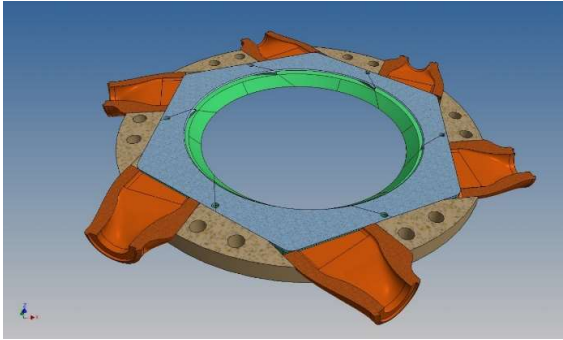


Figure 8. Complete Interface with Injector Ducts (note the changeable blue inserts).

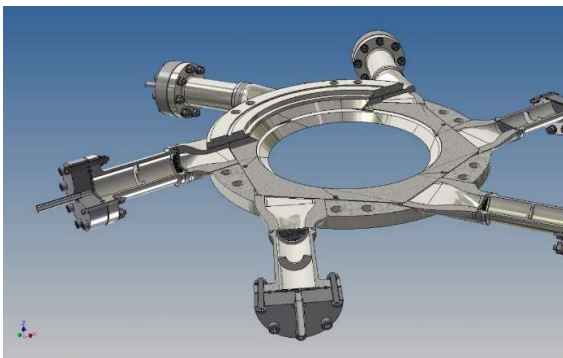


Figure 9. Complete Assembly of Catalytic Injectors and Mechanical Interface.

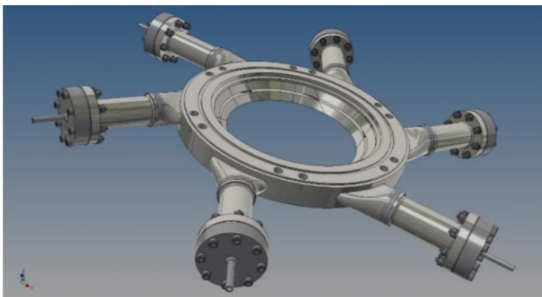


Figure 10. Complete Assembly of Catalytic Injectors and Mechanical Interface.

Finally, two instrumentation ports were designed to accommodate a thermocouple (for one of the decomposition chambers) and a pressure transducer (for its welded injector duct).

5. MANUFACTURE

Manufacturing of all the components described in this paper was the responsibility of DELTACAT. ONERA manufactured the

mechanical interface according to a design agreed between ONERA and DELTACAT.

The ALM machine used for printing the ducts using Inconel 625 was a Renishaw AM250 (see Figure 26). This machine uses powder technology and selective laser melting to produce the parts. The thickness of each printed layer was 60 microns. Seven ducts were manufactured, leaving a spare in case one was needed. The printed ducts were subjected to a light bead blast to remove internal powder and to improve the surface finish. Mass comparisons of the printed ducts are shown in Table 1. It can be seen that consistency in manufacture was very high.



Figure 11. Renishaw AM250 Printer Used for Manufacturing the Injector Ducts.

Table 1. Consistency in Mass for Printed Injector Ducts.

Item	Mass (g)	Deviation from Mean
1	622	0.21%
2	623	0.05%
3	623	0.05%
4	622	0.21%
5	624	0.11%
6	624	0.11%
7	625	0.28%
Mean	623.29	
Maximum deviation	0.28%	

Prior to welding, the injector ducts were X-rayed in accordance with BS M34 to detect any flaws in the printing process. None were found (see Figure 27). Additionally, the alloy was spectrum-analysed, using a Niton XL3t 980 GOLDD+ X-Ray Fluorescence meter, to

confirm that the elemental content was indeed Inconel 625. The elemental content by mass is shown in Table 2; this agrees with the Inconel 625 standard composition UNS designation N06625.

Table 2. Elemental Composition of Printed Inconel 625 (% by mass).

Cr	Mo	Fe	Ni	Nb	Zn	Cu
21.9	8.8	4.2	60.6	3.5	0.10	0.34

The ducts were welded to their respective decomposition chambers using 625 welding material. A complete, welded catalytic injector is shown in Figures 28 and 29. The 5 non-instrumented and one instrumented catalytic injector are shown in Figures 30-32.

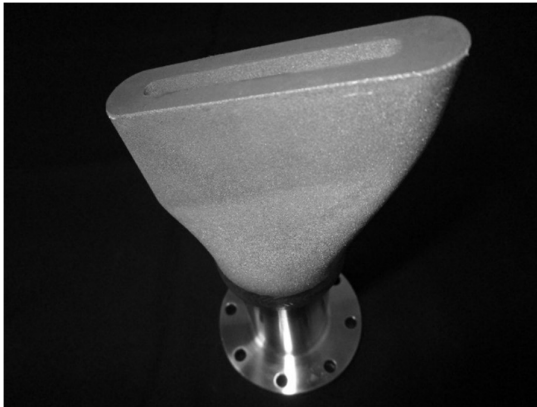


Figure 12. Catalytic Injector Manufactured Using ALM.



Figure 13. Instrumented Catalytic Injector.

6. TESTING

After initial pressure-testing, at a pressure of 30 bar, the catalytic injectors were mounted on the

engine ready for live firing tests. After a short delay with the first firing, the fuel grain ignited and combustion was observed to be steady and sustained (see Figure XX). The temperature of the oxygen being injected was recorded as 880 deg C. The catalytic injectors can now be used routinely for further investigations of optimal fuel grain configurations.

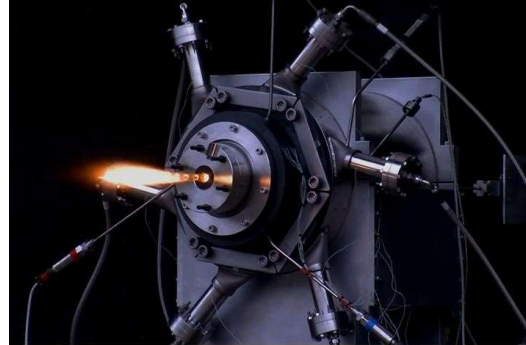


Figure 14. HYPROGEO's Isochoric Hybrid Rocket Engine

7. CONCLUSIONS

This paper has described how the catalytic injector has been designed. Its function is to feed the combustion chamber with oxygen and steam at approximately 900 deg C to provide ignition and sustained combustion of the hybrid fuel grain. A simple regression-rate model has been described; this was validated using data from a pilot experiment. The catalytic injector system has recently been successfully demonstrated in many live firings of the isochoric combustion chamber.

8. ACKNOWLEDGEMENTS

This project has received funding from the *European Union's Horizon 2020 research and innovation programme* under grant agreement No 634534"; the authors are grateful for this support.

REFERENCES

- [1] Odic, K., Lestrade, JY, Verbene, O., Ryan, J., Christ P., de Crombrughe, G., 2016. *HYPROGEO Project Objectives and Coordination*, Paper Number 3124697, Space Propulsion Conference 2016, Rome, Italy.
- [2] Christ, P., Wolf, M. Goek, S., Leininger, S., 2016. *Development of near-anhydrous*

hydrogen peroxide ($\geq 97\%$) for satellite propulsion and assessment of material compatibility for fluidic components and light weight propellant tanks, Space Propulsion Conference 2016, Rome, Italy.

[3] Antony J. Musker, Julia Ryan, Wojciech Florczuk, Kamil Sobcza, Damian Kaniewski, Grzegorz Rarata, Stefan Leininger, Philipp Christ. *Realistic Testing of PX1 Catalyst Using Near-Anhydrous Hydrogen Peroxide*. Space Propulsion Conference, Rome, Italy, 2016.